Effect of Thermal Exposure on Tensile Strength and Microhardness of Welded and Precipitation Hardened RX82 Aluminum Alloy Extrusions in the T4 and T6 Conditions

A Senior Project

presented to

the Faculty of the Materials Engineering Department

California Polytechnic State University, San Luis Obispo

In Partial Fulfillment

of the Requirements for the Degree

Bachelor of Science

by

Lucien Miller

June, 2016

Abstract

This investigation is focused on the effect paint-bake cycles have on the tensile strength and microhardness of GMAW welded RX82 aluminum extrusions in T4 and T6 base conditions. To simulate the paint-bake cycle, T4 and T6 RX82 aluminum samples were GMAW welded and heat treated at 350°F, 390°F, and 425°F for durations of 30 minutes, 1.0 hour, and 2.0 hours, with five replicates for each treatment. Microhardness profiles of T4 samples treated at 350°F for 30 minutes and 1.0 hour display weld/HAZ HV values of 86.04 and 82.51 respectively, followed by maximums of 123.21 and 121.10. Average ultimate tensile strength (UTS) of T4 samples treated at 350°F started at 38.26 ksi, dropped to 34.91 ksi, and increased to 38.24 ksi for 30 minutes, 1.0 hour, and 2.0 hour treatments. T4 samples treated at 390°F showed an increase in UTS with increasing exposure duration; however 425°F treatments displayed a decrease in UTS. T6 samples treated at 350°F and 390°F increased in average UTS, while T6 samples treated at 425°F increased then decreased in strength. A general linear model of the T4 tensile samples shows no statistically significant difference in UTS between treatments or treatment levels, while T6 tensile data shows statistically significant differences between the 350°F and 390°F/425°F treatment temperature, with another significant difference between the 30 minute and 1.0 hour/2.0 hour treatment durations.

Keywords: Aluminum, Heat Treatment, Welding, Precipitation Hardening, Ultimate Tensile Strength, Extrusions, T4, T6, 6082 Aluminum, Materials Engineering

Acknowledgments

I would like to thank Ken Fischer and Dave Lukasak of Sapa Extrusion for their support and sponsorship of this senior project. Their expertise and support was critical throughout the completion of the project. I would also like to thank Luka Dugandzic of Dugandzic Design for assistance with machining samples. Finally, I would like to acknowledge the support and guidance of my senior project advisor Prof. Blair London.

Table of Contents

List of Figures

This portion redacted at request of author.

List of Tables

1. Introduction

1.1 Problem Statement

Sapa Extrusion (Portland, Oregon) supplies aluminum-extruded pieces for use in vehicle frames, such as the Ford F150 and the Jaguar XJ, and support structures, such as the bumper in the Chrysler 200. The extruded parts are typically 6xxx series aluminum and will undergo a variety of treatments prior to installation. These treatments include welding and paint heat treatment. During manufacturing of the vehicles and components there is a possibility for line stoppages in the paint oven cycle, which increases the likelihood of over-aging in the aluminum.

Sapa Extrusion wants to know the effect that thermal exposure has on the mechanical properties of the Heat Affected Zone (HAZ) in their welded T4 and T6 RX82 aluminum alloy extrusions. Research indicates that when 6xxx series aluminum alloys are exposed to elevated temperatures, after being aged to the T4 and T6 conditions, that the alloy will have decreased yield strength and hardness. The effect of elevated temperature exposure on welded sections of 6xxx series aluminum has yet to be studied and is the purpose of this experiment. In this project, welded T4 and T6 RX82 samples will be exposed to a variety of elevated temperatures (350°F, 390°F, 425°F) for differing amounts of time (30 mins, 1 hr, 2 hrs).

Tensile testing a variety of welded and heat treated RX82 samples will produce data that can be statistically analyzed to determine the average effect elevated temperature exposure has on tensile properties in the HAZ of the weld. Microhardness profiles of the welded region in over-aged samples will show the effect post weld heat treatment has on the microstructures present throughout the HAZ. Performing these tests and statistically analyzing the results will aid Sapa Extrusion in designing their extrusions for use by consumers.

1.2 Background

1.2.1 Company Background

Sapa Extrusion is a recent merger of two aluminum companies, Orkla ASA and Hydro ASA. Sapa's company goal is to shape a sustainable future through innovative aluminum solutions [1]. If there exists a heavy steel part, it is likely that Sapa can replace that part with an aluminum extrusion, resulting in weight savings while maintaining strength and quality. As the

automotive industry looks for ways to reduce their overall greenhouse gas footprint, Sapa offers a solution in producing light-weight extrusions that can be assembled into a variety of automotive components. The demand for all aluminum car components has prompted Sapa to dedicate one of their extrusion plants solely to the automotive industry [1]. Sapa Extrusion has also begun working with electric vehicle manufacturers in the pursuit of reducing the impact the automotive industry has on greenhouse gas production.

1.2.2 Aluminum Alloys in the Automotive Industry

Aluminum is a highly abundant metallic element in the earth's crust. Aluminum ore always occurs as a compound, such as bauxite, which is the basic raw material from which the metal aluminum is produced. The bauxite ore is then processed into a variety of aluminum alloys through chemical reduction processes.

Aluminum alloys are desirable materials to use in structural applications because of their high strength-to-weight ratio. They are also easily machined and extruded, have good corrosion resistance, good thermal and electrical conductivity, and are heavily recycled. These desirable properties are the reason aluminum's use has recently increased in the automotive industry. The Ford F150 and the 2010 model of the Jaguar XJ all have a large percentage of their body and frame made of extruded aluminum. In the Jaguar XJ, the cantrail is made from a combination of hydroformed and extruded parts that are assembled together. The change from steel to aluminum parts saves 7.4 lbs of weight from the cantrail. Jaguar reports in their life cycle analysis of the cantrails a CO_2 reduction of 3,452 tons over the car's lifetime [1]. The 2015 Ford F150's aluminum body reduces the total vehicle weight by up to 700 lbs (**Figure 1**).

Figure 1 - The 2015 Ford F-150 body is made entirely of aluminum extrusions. Producing the body out of aluminum as opposed to steel reduces the weight of the body by 700 pounds while improving its corrosion resistance and strength-to-weight ratio [1].

1.2.3 Sapa's RX82 Aluminum Alloy

RX82 is a Sapa Extrusion proprietary 6xxx series aluminum alloy composed primarily of aluminum with significant additions of silicon, iron, copper, manganese, magnesium, chrome, zinc, and titanium [2]. Its composition falls within the specifications of a 6082 aluminum alloy, but Sapa's RX designation signifies that the alloy undergoes recrystallization during the extrusion process. Essentially, the heat generated by the stresses of extrusion results in the alloy exceeding its solvus line, which enables the alloying elements to diffuse throughout the now single phase billet, increasing the homogeneity of the billet for future processing.

1.2.4 Aluminum Extrusion

The process of extruding aluminum begins with the casting of ingots or billets. Initially, the melt is formed from mixing different feed streams in a furnace to acquire a final specified composition. The melt is then gravity fed into molds, where the aluminum begins to cool and crystallize. Initially, the increased cooling rate at the cast walls causes crystals to nucleate heterogeneously. As the billet cools the grains grow towards the center of the casting, impinging on each other to form grains. The growth of these aluminum rich grains forces the alloying elements to diffuse towards the grain boundaries.

After the billet is cast, it is solution heat treated above its solvus line to homogeneously distribute the alloying elements throughout the material . This step not only facilitates future strengthening through the formation of precipitates, it also increases the extrudability of the billet due to alloying elements not forming hard precipitates along grain boundaries [3], [4].

This portion redacted at request of author.

The solution heat treated billet is then ready to be fed into the extrusion process. Extrusion is the process of forming profiles by using pressure to force a material through a set of dies. This process utilizes plastic deformation to form extrusions that have consistent cross-sectional profiles and wall thickness. There are two types of extrusion, direct and indirect (**Figure 3**). For this application Sapa Extrusion uses direct extrusion, where a compressive force is used to push the RX82 billets through a die. These compressive stresses help to ensure that there is no cracking in the billet during extrusion [5].

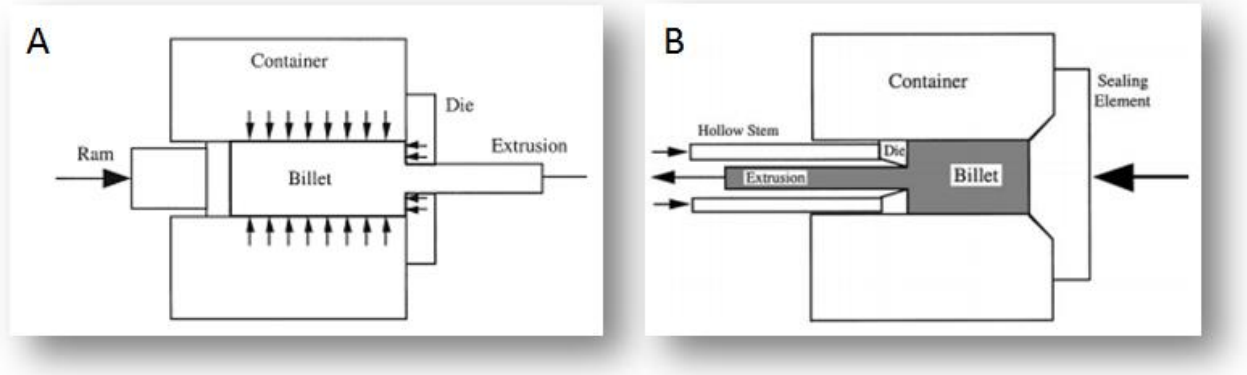

Figure 3 – Schematic showing **(A)** direct extrusion and **(B)** indirect extrusion. The compressive forces on the billet are shown in the direct extrusion schematic. The stem being pushed into the container as the extrusion gets pushed out the opposite side is shown on the indirect extrusion schematic [5].

As the billet is being forced through the extrusion die, the friction generated between the two contacting surfaces generates enough heat to bring the billet above its solvus temperature. This is what the RX82 alloy was made for, because the heat generated not only serves to dissolve the Mg_2Si precipitates and form more ductile alpha phase, it also allows the extrusion to recrystallize upon being extruded. The extrusions are quenched immediately to form a super-saturated solution that can be aged to form strengthening precipitates. The extruded aluminum profiles (**Figure** 4) are cut to length and moved to a secondary stretching process. The stretching relieves stresses in the material and gives the profiles their desired straightness [6].

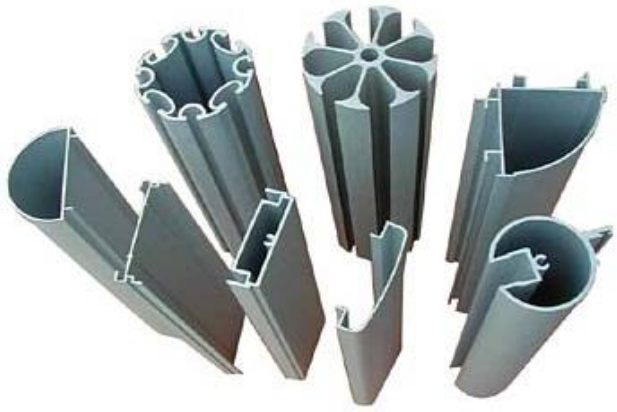

Figure 4 - An aluminum profile is the specific shape of the extruded metal after it is pushed through the die. Companies such as Sapa have thousands of different dies for profiles that may be used in many applications. Most dies are custom made for a specific profile and a specific application [1].

1.2.5 Precipitation Hardening (Age Hardening)

Age hardening is the stage during which the strength and ductility of the aluminum extrusions are optimized [1]. Age hardening is the process of growing precipitates within an alloy for the purpose of inhibiting dislocation movement. Precipitate formation is initiated at locations within the sample where there is sufficient potential energy for the alloying element atoms to aggregate and form intermetallics like Mg_2Si. This growth can occur naturally at room temperature, but may require long periods of time to achieve a stable precipitate size where the material is classified as T4. Artificial aging (T6) is a process where an extruded profile is placed in an oven around 350°F, expediting the growth of precipitates and producing a measurable increase in strength [6].

Precipitates are the final result of numerous kinetically and thermodynamically enabled processes that take place during aging. Initially, the Mg and Si atoms cluster near grain boundaries. This is followed by the formation of Guinier-Preston (GP) zones. The GP zones grow and form the ß″ intermediate precipitate. With further aging the ß′ forms from the ß″ precipitates. Eventually the equilibrium ß-Mg_2Si phase is formed.

The ß″ precipitates are coherent with the aluminum matrix, the ß′ precipitates are semi-coherent, and the ß-Mg_2Si are incoherent. When the precipitates are small and coherent with the aluminum matrix, dislocations shear through the precipitate, adding a small amount of strength to the material. As the incoherency of the precipitates increases due to elevated temperature and time, the dislocations have to bow around the precipitate. The top of the peak (**Figure 5**) is referred to as the peak age condition, and is where the maximum strength of the material is found [4].

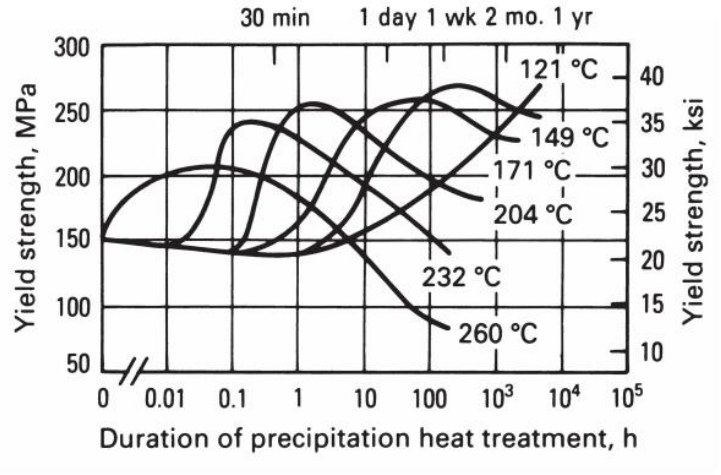

Figure 5 - A diagram of the impact that precipitation aging duration, as well as aging temperature, have on the yield strength of a 6061 aluminum alloy [7].

Past this point where the equilibrium phase is reached is known as overaging. Before the peak where the ß″ phase is present is known as underaging. Overaging results in a loss of strength because as the precipitates grow larger, and the overall amount of precipitates in the system lowers as a result of Ostwald Ripening. Ostwald ripening is a thermodynamically-driven spontaneous process in which smaller precipitates begin to dissolve and redeposit onto larger crystals thus decreasing the overall surface area of the precipitates. As the precipitates continue to grow, the distance between them increases. Eventually they are so far apart that, for all intents and purposes, diffusion no longer occurs, and the strength of the alloy ceases to change. Over-aging can occur even after heat treatment if the material is exposed to any other considerable source of thermal energy, such as the heat generated from welding or curing powder coat paint.

1.2.6 Welding of 6xxx Series Aluminum

The process of welding aluminum is relatively tricky due to the considerations that must be taken prior to joining the two components. For RX82 aluminum, the weld surfaces must first be properly prepared. If there are any oxides present on the surface of the extrusion prior to welding, or if any form during welding due to oxygen reacting with aluminum to form alumina, the oxide can sink into the weld pool. These oxides can form inclusions, and greatly reduce the strength of the joint [8]. To join the two surfaces with Metal Inert Gas (MIG) welding, the welder must select a filler metal suitable for the given application. 4xxx series aluminum filler metal is used to join most age hardenable aluminum alloys, like RX82, but it shouldn't be used in

applications where the joined pieces are anodized due to formation of grey streaks resulting from the silicon precipitating out of the joint. An Al-Mg alloy filler metal is used in applications where greater strength is desired [1].

After welding, the joint is usually heat treated to ensure there is sufficient strength in the joint and the HAZ surrounding the weld. This is done because the process of welding drastically alters the microstructures present in the extrusion surrounding the welded joint. The process of welding produces a cast structure in the weld pool. Extending outward from the midline of the weld entering the parent material, the HAZ is comprised of a solutionized zone, an annealed zone, an overaged region, and finally transitioning to unaffected base metal [1]. The cast structure and the annealed zones are the weakest and softest areas (**Figure 6**), and it is here that fracture usually occurs during tensile loading [1], [9].

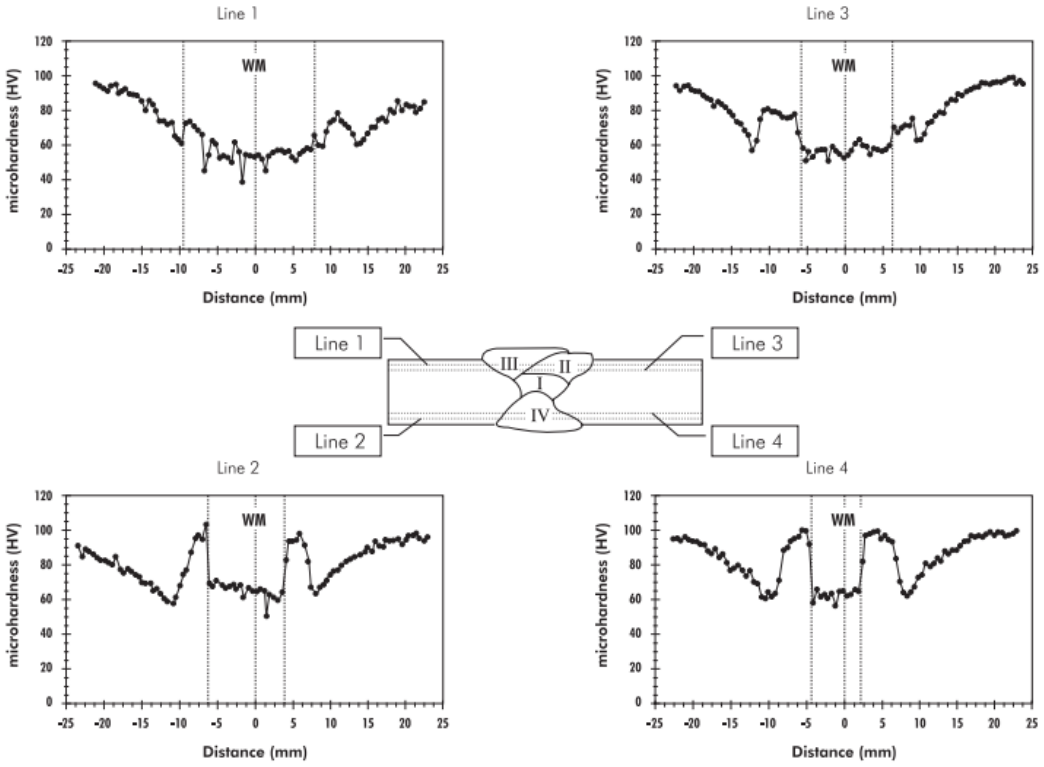

Figure 6 – Taken from a study investigating the mechanical behavior of 6082-T6 aluminum alloy welds, this Vickers microhardness profile reveals that the softest areas are within the weld pool and a small distance outside of the weld pools [9].

RX82 is an alloy that is strengthened through the use of precipitates inhibiting dislocation movement; however these strengthening precipitates are thermodynamically unstable when exposed to welding conditions. As RX82 is being welded, the smaller ß″ precipitates will begin to dissolve when the local HAZ temperature exceeds 480°F, while larger precipitates grow. Closer to the weld fusion line the ß″ precipitates can undergo reversion. In the HAZ where temperatures range from 480-900°F coarse ß′ can form and rapidly grow due to the increased solute content from the smaller dissolving ß″ precipitates. These microstructural changes ultimately affect the yield strength and hardness throughout the welded, heat affected, and base metal zones. Post Weld Heat Treatment (PWHT) of the component after welding can recover some of the strength lost through the process of welding. During PWHT, ß″ will precipitate and grow in the regions that underwent reversion during welding. The ß″ reversion is most extensive in areas of high solute content near the weld fusion line (Figure 7) [10].

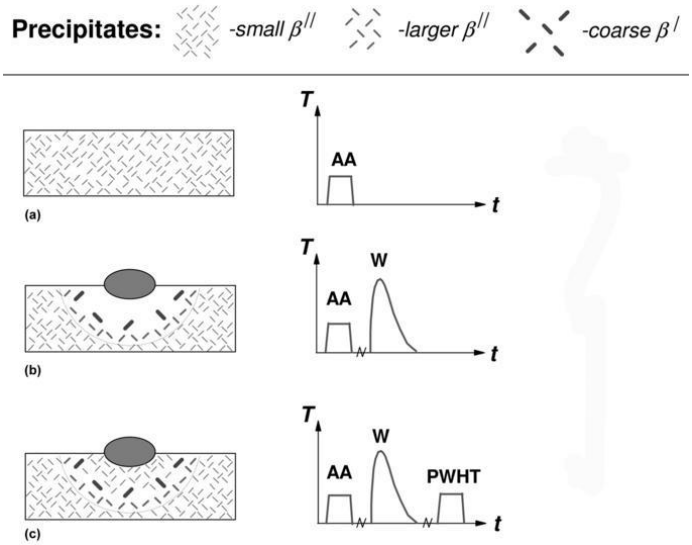

Figure 7 – The microstructures present in Al-Mg-Si alloys after various processes. (a) The microstructure following Artificial Aging (AA) is predominantly ß″. (b) When welded, some ß″ dissolves and is replaced by weld metal and coarse ß′. (c) PWHT recovers ß″ precipitates, recovering strength in the HAZ [10].

1.2.7 Powder Coating Aluminum

In the automotive industry, coating is a common practice used to improve the surface properties of a component, as well as improving its aesthetics. There are two main methods of coating metallic components, powder coating and wet coating. While the material costs are

similar between powder and wet coating, savings in operational cost make powder coating a more efficient coating process [11]. Powder coatings are paint films composed of a structural binder, pigment, and additional additives. The structural binder is composed of a resin and polymer. The pigment and additives affect the aesthetics, fluidity, and application properties of the coating [12].

In the automotive industry, electrostatic spray is the most common powder coat application process. A spray gun is used to electrostatically charge the hopper supplied powder, which is then sprayed onto the grounded component (**Figure 8**). After the coating has reached a desired thickness on the material surface, the coated component is transferred to an oven for curing. Inside of the oven the temperature is above the melting point of the powder. The coating film is formed by powder particles melting, flowing, and fusing to the component surface [13]. The powder coating process takes approximately 30 minutes at 350°F; however this can vary based on the temperature of the curing conditions.

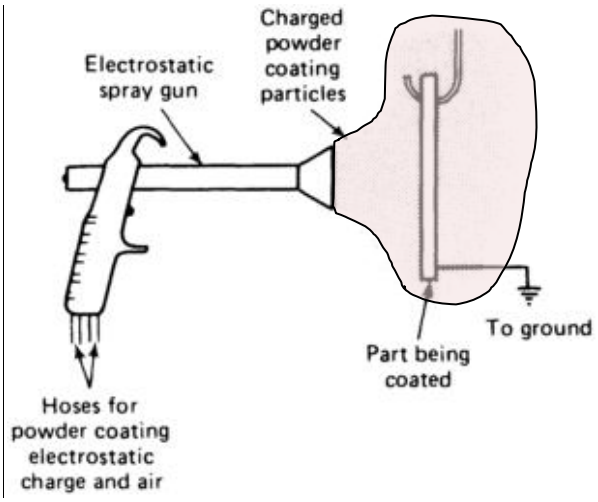

Figure 8 – The process of powder coating aluminum involves spraying electrostatically charged powder onto a grounded component [13].

1.3 Previous Research on Similar Topics

1.3.1 Perforation of welded aluminum components: Microstructure-based modeling and experimental validation

A study investigating the effect MIG welding has on the mechanical properties of AA6082 – T6 shows that the process of welding reduces the strength of the component in the weld pool and HAZ. In this study, 10 mm, 20 mm and 30 mm thick extrusions made of

AA6082-T6 were MIG welded with Safra 5183 welding wire. The 10mm extrusions were welded with three passes, while the 20mm extrusions received eight passes, and the 30mm extrusions received twelve passes.

Three tensile tests were performed on the base material in both the direction of extrusion and the cross-weld direction. For these tests, there was not any substantial difference in yield strength. Microhardness profiles of the weld region and HAZ were gathered, through Vickers hardness testing, to pinpoint the location of the HAZ as well as identifying the differences in strength caused by MIG welding (**Figure 9**). The microhardness profiles indicated that the weakest portion of each sample was in the area between the weld pool and the base metal [14].

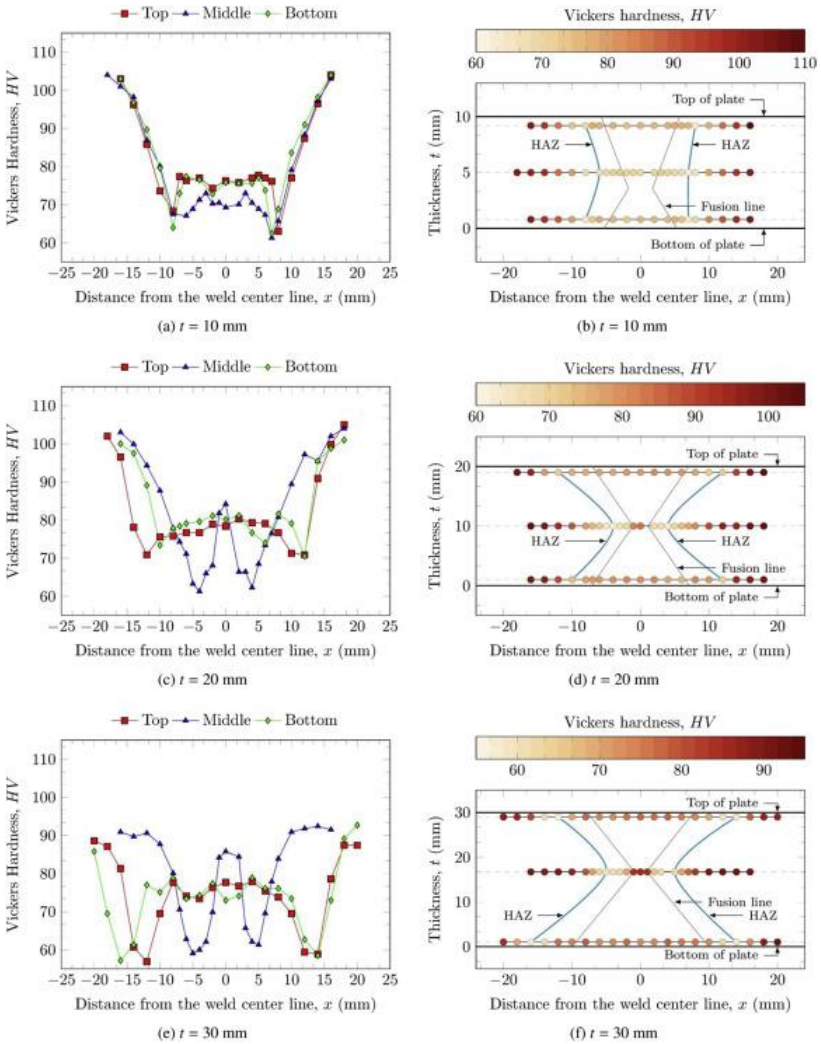

Figure 9 – The microhardness profile of MIG welded AA6082-T6 extrusions. The profiles vary in thickness from 10mm to 30mm. Each sample was tested along three lines through the weld. All samples show a minimal hardness in the HAZ of their weld [14].

2. Experimental Procedure

2.1 Production Sample

2.1.1 Bumper Reinforcement Sectioning

Sapa Extrusion provided an example of the welded and painted specimen in the form of a Chrysler 200 bumper reinforcement. This product consisted of a main RX82 extruded profile that was fillet welded to two separate crash cans. The bumper was provided to be sectioned for microhardness analysis of base metal and weld profiles. Luka Dugandzic of Dugandzic Design (San Luis Obispo, CA) was contracted to produce general sections of the welded region that could be further processed for metallographic mounting and microhardness testing. Initially, a portion of the RX82 profile was sectioned using a horizontal metal band saw, enabling further cuts to be made on the crash can (**Figure 10**). This reduced portion of the reinforcement was then cut along the longitudinal direction of the extrusion, separating the rear weld bearing face from the front of the profile. Nine cuts were then made in the longitudinal and transverse directions to section the welded portion of the extrusion.

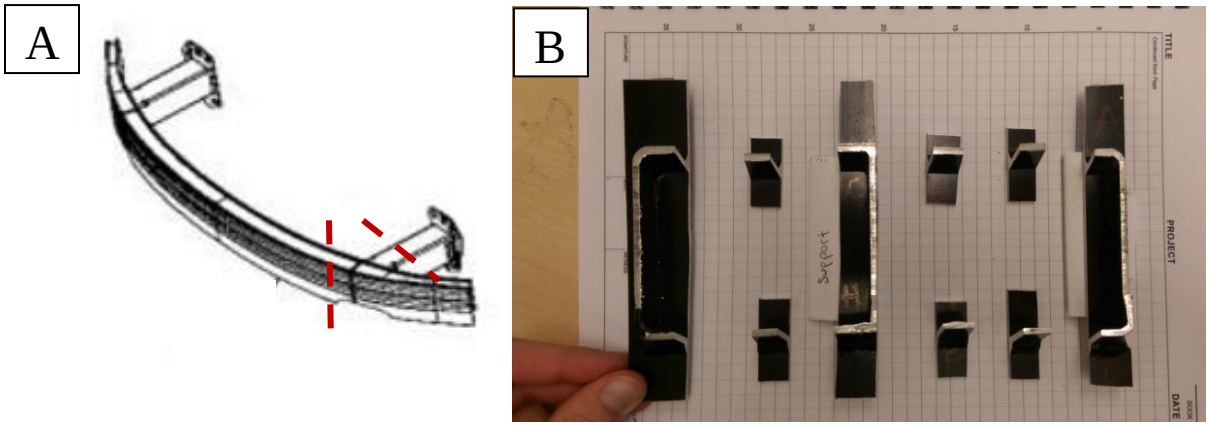

Figure 10 – (A) The schematic of a production Chrysler 200 bumper reinforcement. The dotted lines indicate general sectioning cuts that were made to expose the weld for further sectioning [15]. **(B)** The resulting sections that were eventually cut using a wafering blade.

Using the sections obtained from Dugandzic Design, further processing was performed to reduce their size in order to fit them into the 1-1/4 inch diameter acrylic mounts. Longitudinal and transverse samples were sectioned by an Allied Techcut 4 with a lubricated wafering blade spinning at 130 RPM.

2.1.2 Section Preparation

After the weld samples were cut to size, they were mounted in acrylic following standard procedure. The resulting samples were then ready for rough polishing on 240, 320, 400, and 600 grit abrasive papers, followed by polishing on 6 micron and 1 micron pads with diamond colloidal solution. Samples of unaffected base metal were obtained from the bottom flange of the RX82 extrusion using the same wafering, mounting, and polishing procedures (**Figure 11**).

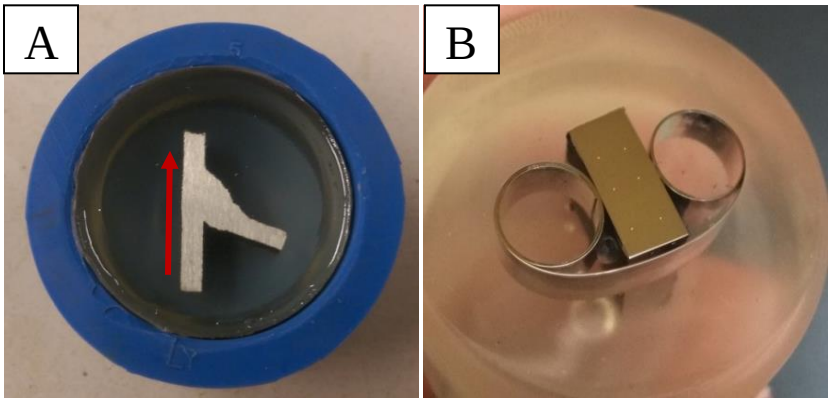

Figure 11 – **(A)** A transverse sample of weld metal from a Chrysler 200 bumper reinforcement mounted in acrylic for microhardness testing. Indentations were made along the red arrow. **(B)** A transverse section of base metal mounted using the same material and procedure as the weld section. The small indentations are Vickers microhardness indentations.

2.1.3 Microhardness Indenting

Following sample surface preparation, Vickers microhardness indentations were made to determine the hardness of weld profiles as a function of distance from the weld, as well as the relative orientation of the weld and extrusion direction. Vickers indentations were taken following ASTM Standard E384 – 11E1 *Standard Test Method for Knoop and Vickers Hardness of Materials* [16]. From the ASTM specifications, it was determined that indentations should be made using 500 grams of force for a load time of 10 seconds. Testing was conducted using a Buehler Micromet II Microhardness Tester. Microhardness indentations on the weld specimens were placed 0.05 inches apart, running the length of the base extrusion (**Figure 11 A**). Six indentations were made on the sections of unaffected base metal in order to determine their average hardness.

2.2 Main Experiment

Sapa Extrusion MIG welded plates of T4 and T6 base extrusions. The extrusions were welded along their transverse faces, enabling tensile testing to be conducted in the longitudinal direction. 50 tensile samples were milled from the MIG welded T4 plates, while 45 were milled from the T6 plates. The samples were shipped from Sapa production facilities in Detroit, MI to San Luis Obispo, CA for treatment and testing. Samples arrived in the as-welded condition.

2.2.1 Sample Treatment

Sample treatment was conducted using a low temperature oven in the Cal Poly Materials Engineering Department's Heat Treatment Lab. Sample treatment temperatures and times were based around last year's Sapa Extrusion senior project that investigated the effect of coating treatments (specifically paint-bake cycles) on the tensile strength of a variety of extruded aluminum alloys [17]. It was found that treatment temperatures of 350°F, 390°F, and 425°F simulate the temperatures that car components may experience during a run in a production scale curing oven. Treatment durations of 0.5, 1.0, and 2.0 hours were used to completely cover the duration of a paint-bake cycle, in addition to having larger durations that account for any stoppages in the oven (**Table I**)

Table I – Thermal Exposure Experimental Treatments

		Duration (hr)		
		0.5	1	2
Temperature (°F)	350	T4	T4	T4
		T6	T6	T6
	390	T4	T4	T4
		T6	T6	T6
	425	T4	T4	T4
		T6	T6	T6

Prior to sample treatment an oven survey was conducted to ensure that the internal temperature of the oven would remain within a ±10°F range. Following confirmation of oven reliability, a PWHT was applied to the T4 samples. This treatment at 350°F for five hours was done to replicate Sapa Extrusion's standard procedure for producing welded components that start in the T4 condition. Initially the oven was heated to 350°F while the samples were loaded onto trays, with thermocouples attached to the left and right of each tray. Once the oven reached 350°F the samples were loaded. Once the thermocouples indicated that the samples had reached 350°F, a timer was set for five hours. Upon completion of the PWHT the T4 samples were removed from the oven and still air cooled on bricks, with the gage length exposed to facilitate air circulation around the welded region (**Figure 12**). Experimental treatment of the T4 and T6 samples followed the same procedure of oven heating, sample loading, and cooling. Nine different treatments were applied to both the T4 and T6 samples, with five replicates for tensile testing and no replicates for microhardness profiles.

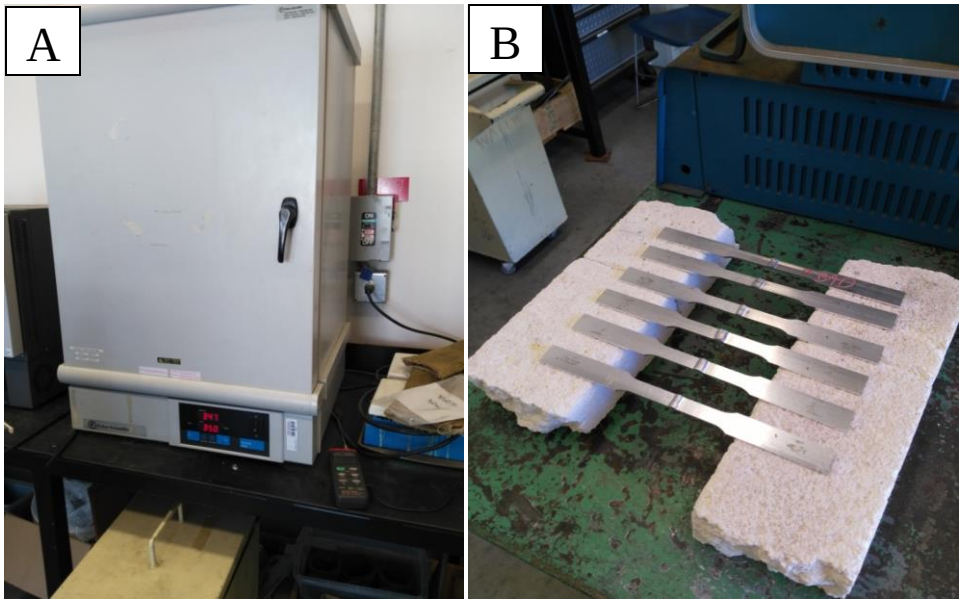

Figure 12 – (**A**) The low temperature oven used to treat the T4 and T6 RX82 samples. At the bottom right of the oven is the thermocouple and datalogger used to monitor the internal temperature of the oven. (**B**) Samples were still air cooled after treatment in the oven. The gage length is exposed in order to facilitate even cooling around the weld.

2.2.2 Tensile Testing

The main form of characterization employed was the use of an Instron 5545 Tensile Tester with a 150kN load cell. ASTM Standard B557 - *Standard Test Methods of Tension Testing Wrought and Cast Aluminum- and Magnesium-Alloy Products* was used to determine

appropriate testing variable values, such as crosshead displacement rate [18]. The samples had an average gage thickness of 0.10 in and an average width of 0.498 in. Samples were tested with a cross-head displacement rate of 0.10in/min. Maximum load was recorded to determine the ultimate tensile strength of each sample.

2.2.3 Microhardness Indenting

Samples that were used for microhardness indentation were sectioned using the same wafering blade setup employed in the sectioning of the production sample. The samples were sectioned down the midline of the weld to expose the transverse view of the weld and HAZ. Sections were cold mounted in acrylic and polished to 1 micron.

As stated in the production sample section, Vickers microhardness indentations were made using a Buehler Micromet II Microhardness Tester, a Vickers indenter, and 500 grams of force for a load time of 10 seconds. Indentations were made from the midline of the weld outwards to the unaffected base metal at intervals of either 0.01 inches or 0.02 inches.

3. Results

3.1 Production Sample

After indentation, the diagonal lengths of the indentations were measured to the nearest 0.5 micron (**Figure 13**). Measurements were performed using a calibrated eyepiece on the Buehler testing apparatus. The indentation was located and focused at 40X magnification, followed by horizontal and vertical measurement of the diagonal lengths. The two lengths were averaged, and the HV Vickers hardness was calculated.

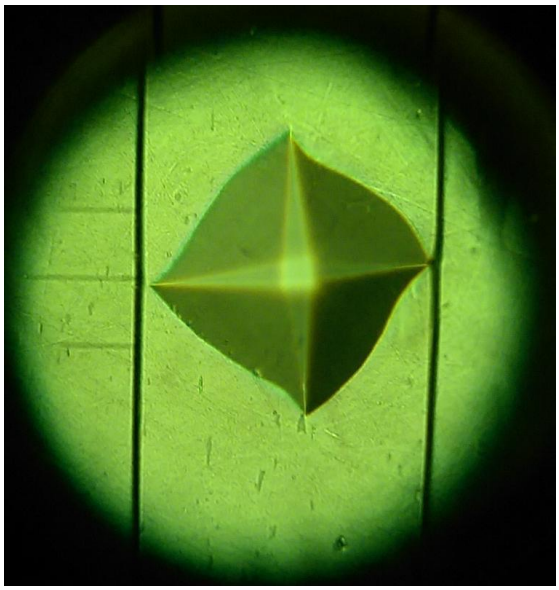

Figure 13 – A Vickers indentation made on the surface of the transverse production weld sample. The black bars are the outside boundaries that were used to measure the diagonal lengths of the indentation in order to calculate the microhardness.

From the data gathered, profiles for the transverse (**Figure 14**) and longitudinal **(Figure 15)** samples were developed. Both samples show maximum hardness values that lie in the base metal region, while there is a stark decrease in hardness as the profile comes closer to the weld.

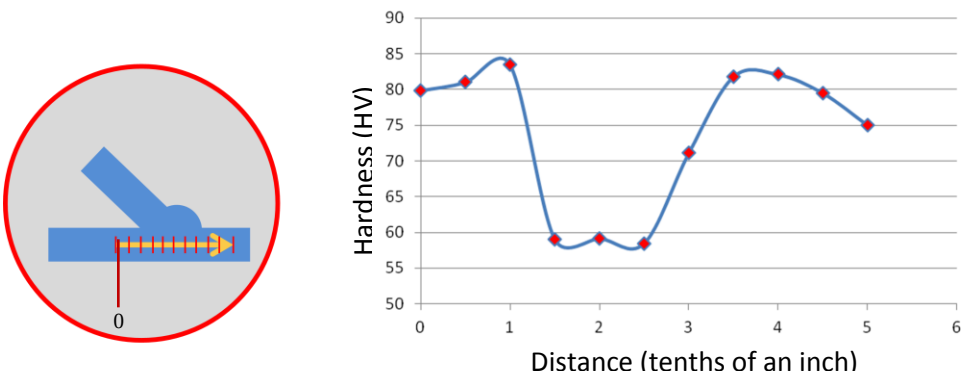

Figure 14 – The microhardness profile for the transverse weld section from the production sample. HV values start around 80 in the base metal, drop to 58 in the welded region, then return to 75.

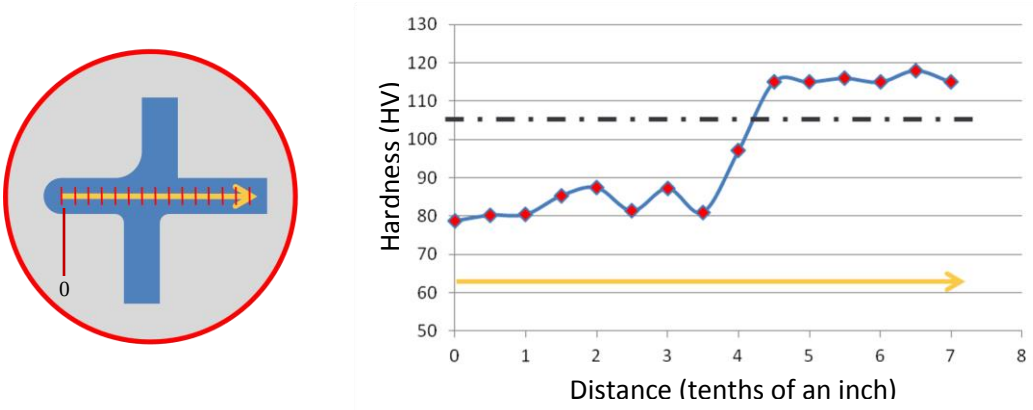

Figure 15 - The microhardness profile for the longitudinal weld section from the production sample. HV values start around 80 in the base metal near the flange and maintain this hardness through the welded region, then reach a maximum of 115.

3.2 Tensile Test Results

Tensile testing generated curves of tensile stress as a function of sample extension. These figures were visual representations of the effect that thermal treatments may or may not have had on mechanical properties (**Figure 16**).

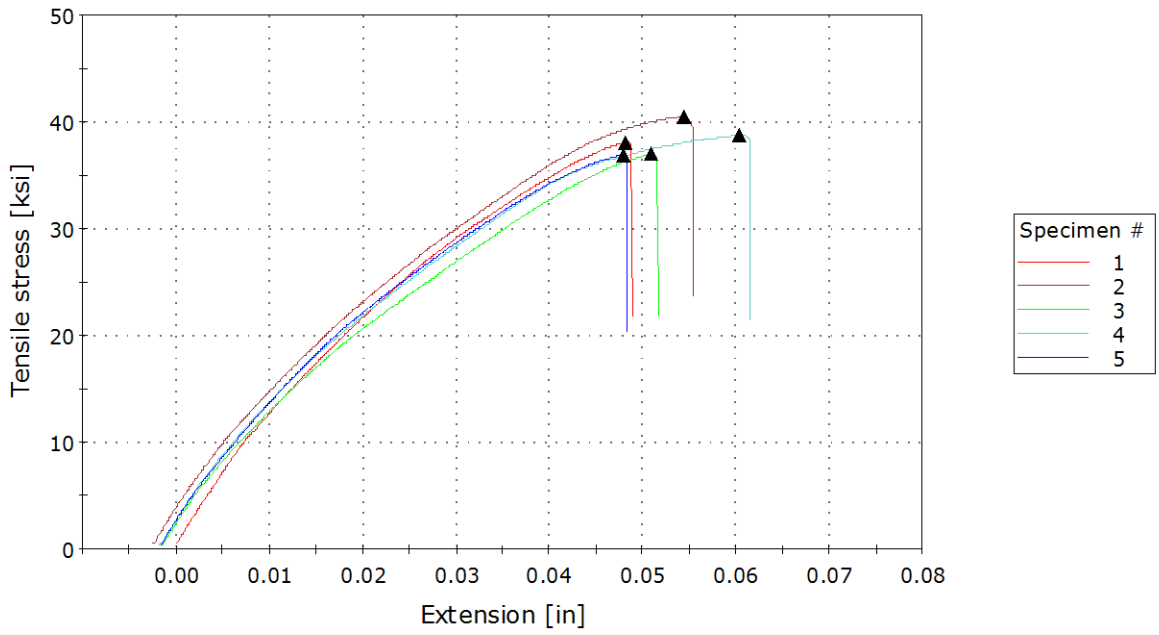

Figure 16 – A stress-extension graph of T4 samples that were treated at 350°F for 0.5 hours. All of the samples appear to be failing around the same tensile stress.

The ultimate tensile strength of each sample was calculated by dividing maximum load supported by the cross-sectional dimensions of the tensile sample near the base of the weld bead (**Table II** and **Appendix A**). Almost all of the samples failed in the area next to the weld bead, however there were a few exceptions where the sample failed between the weld bead and the end of gage length. These failures had substantially larger reductions in area than the samples that failed by the weld bead, yet they had similar maximum loads. Graphical analysis of the data sets was completed by averaging the UTS for each treatment group, then plotting UTS as a function of treatment duration, with results grouped by treatment temperature (**Figures 17** and **18**).

Table II – Average UTS Values in ksi For Thermally Treated Samples

Temper	Treatment Temperature (°F)	Treatment Duration (hours) 0.5	1	2
T4	350	**38.26**	**34.91**	**38.24**
	390	**36.74**	**37.65**	**37.77**
	425	**37.10**	**36.22**	**35.36**
T6	350	**28.39**	**30.31**	**30.68**
	390	**30.99**	**34.99**	**36.78**
	425	**30.77**	**33.67**	**32.95**

There is a large amount of variation in the average UTS of the T4 samples with no apparent relationships between treatment temperature and duration (**Figure 17**). The 350°F treatments start over 38 ksi, drop to 35 ksi after 1.0 hour of treatment, then increase to 38 ksi at 2.0 hours, Increasing treatment temperature to 390°F from 350°F for the 0.5 hour treatments results in a decrease in average UTS. The 390°F group shows increasing strength with increasing treatment duration. This trend is reversed for the 425°F treatments, which show a decrease in UTS with increasing treatment duration.

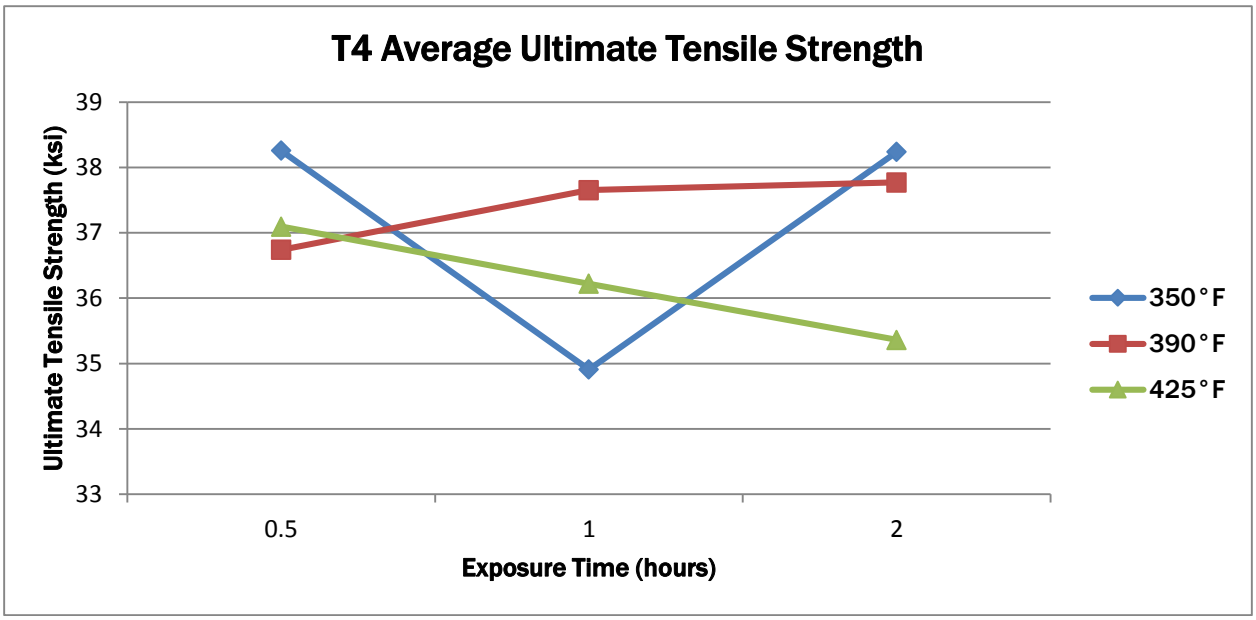

Figure 17 – The average UTS results from T4 samples that were thermally treated. There is not any apparent correlation between treatment factors and changes in UTS.

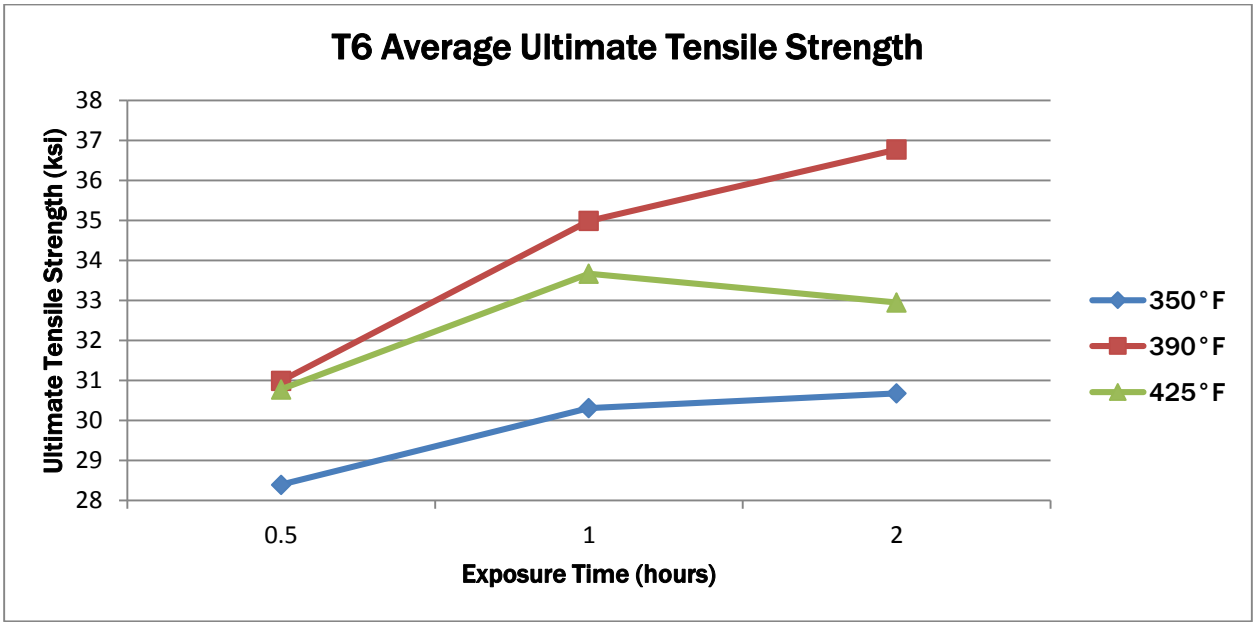

Figure 18 – The average UTS results from T6 samples that were thermally treated. UTS appears to increase with increasing treatment temperature and time, however there is a later decrease in UTS of the 425°F treatment group, and UTS decreases as temperature increases from 390°F to 425°F

Initial graphical analysis of the T6 data shows that increasing treatment duration leads to an increase in UTS, with the only exception being the increase from 1.0 hour to 2.0 hours in the 425°F treatment group (**Figure 18**). There is also an increase in UTS from 350°F treatments to 390°F treatments. Going from 390°F to 425°F, however, results in a slight decrease in strength, but with average values that still exceed the 350°F treatment group. The combination of the observations between treatment temperature and duration affected UTS indicates that a process limitation was observed. Paint-bake cycles operating at 390°F appear to be the optimal temperature for strength recovery in the welded region. Based on the trend observed in the 425°F treatment group, it can be surmised that if the treatment duration of the 350°F and 390°F treatments were increased beyond a certain point, an eventual decrease in strength would be observed. The process limitations of temperature and time could be manifestations of overaging and Ostwald Ripening.

3.3 Statistical Analysis of Tensile Results

Statistical analysis of the T4 and T6 UTS values was conducted using MiniTab software. Prior to conducting an analysis of variance, both T4 and T6 data sets were tested for equal variance. The T4 group passed Bartlett's test with a P-value of 0.004. The T6 group was less conclusive, producing a P-value of 0.083. These tests were followed by an analysis of variance utilizing a General Linear Model (GLM). Using this form of analysis in conjunction with Tukey intervals enables detailed analysis of the effect of each factor, as well as differences caused by each factor level.

GLM analysis of the T4 group produced P-values to determine whether treatment temperature or time cause statistically significant differences in UTS. The samples were also tested to see if there was any interaction between these two factors. The P-values for temperature and time were 0.205 and 0.239 respectively. Since these values were larger than the threshold value of 0.05, we cannot confirm that these factors cause statistically significant changes in UTS. The T4 samples therefore have the same UTS regardless of the thermal treatment they were exposed to. The P-value for the interaction between factors was found to be 0.041; however the interactions plot simply shows that the two factors had a synergistic effect on UTS, with no correlation between increases or decreases in UTS with changes in the factor levels (**Figure 19**).

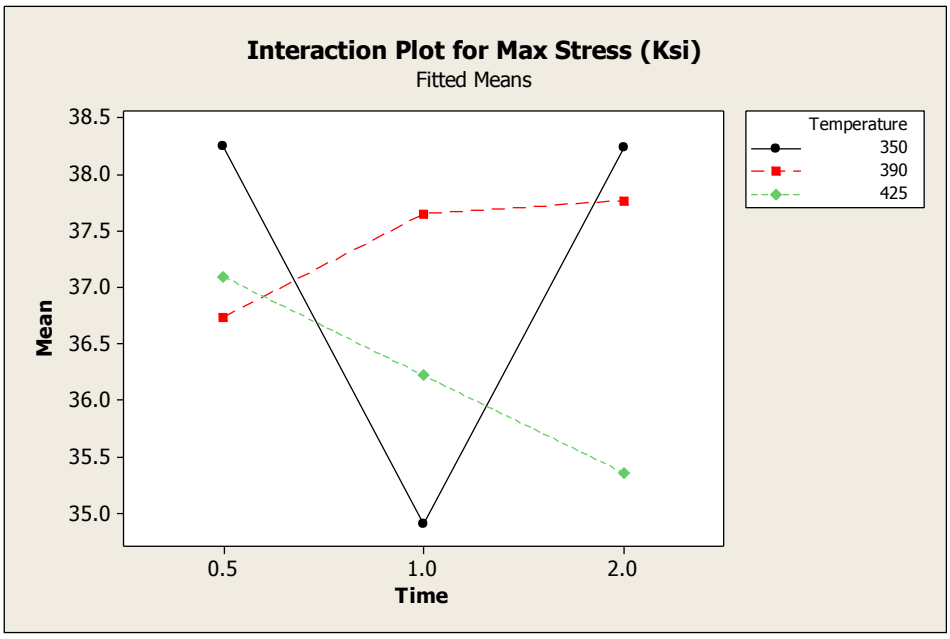

Figure 19 – An interaction plot of the temperature*time effect on the UTS of T4 samples shows that while there is a synergistic effect on strength, the effect cannot be determined to be strictly positive or negative.

Analysis of T6 data produced more conclusive results. A GLM was used, testing for the same factors, factor levels, and interactions used in the T4 analysis. The treatment temperature, time, and interaction had P-values of 0.000, 0.002, and 0.518 respectively. From this, it can be determined that treatment temperature and time had a statistically significant effect on UTS, which means the UTS of welded T6 RX82 does vary with thermal treatments. The Tukey grouping within factor levels indicated that the 350°F treatments had UTS values that were significantly lower than samples treated at 390°F and 425°F. The 390°F treatments had an average UTS value that was 4.56 ksi higher than the 350°F treatments. The 425°F treatments had UTS values that were 2.67 ksi higher than 350°F treatments. Characterizing the graphically observed difference in strength between the 390°F and 425°F treatments was an average decrease in UTS of 1.79 ksi. This decrease is not statistically significant because there is an overlap in the 95% confidence interval (CI) of the difference in mean UTS values, meaning that there is a chance that the samples have the same mean UTS value. Tukey grouping also determined that the 0.5 hour treatments were significantly lower in UTS than the 1.0 and 2.0 hour treatments. The 1.0 hour treatments had mean UTS values that were 2.94 ksi higher, while

2.0 hour treatments were 3.42 ksi higher. Similar to the higher treatment temperatures, the higher treatment times included a possible overlap in mean UTS values; however the middle of the 95% CI indicated a mean increase of 0.48 ksi when time was increased from 1.0 to 2.0 hours.

3.4 Microhardness Profiles

Employing the same methods that were used in the analysis of the microhardness profiles for the production sample, the indentation lengths were tabulated, averaged, and converted to microhardness (**Appendix B**). The T4 samples treated at 350°F appear to have little to no deviation in regards to microhardness maximum/minimum values, as well as no changes in extent of the HAZ (**Figure 20**). This behavior is as expected, due to the samples being post-weld heat treated at 350°F for five hours prior to any experimental treatments.

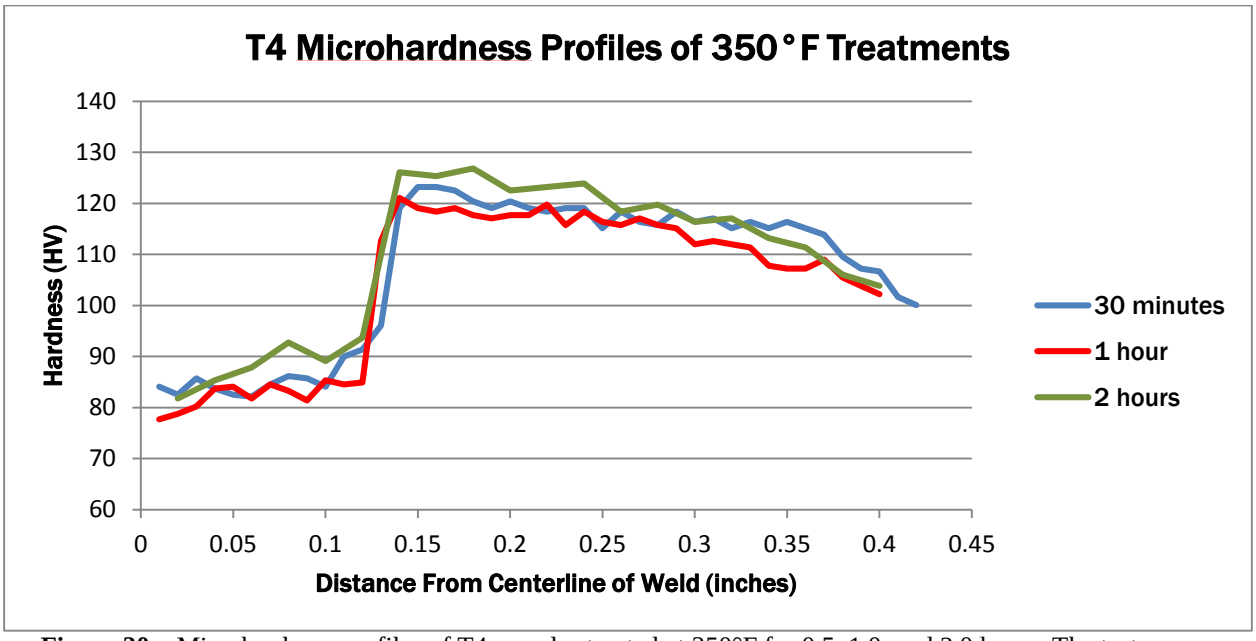

Figure 20 – Microhardness profiles of T4 samples treated at 350°F for 0.5, 1.0, and 2.0 hours. The tests were performed in the transverse direction, starting in the weld metal and moving outwards to the unaffected base metal.

T4 samples that were treated at 390°F produced different results. Not only were there substantial differences between maximum and minimum values, there was also a large variation in extent of the HAZ. These changes also did not appear to follow any trend related to treatment duration. This could be the result of changing indentation steps from 0.01 inches to 0.02 inches, however further testing would need to be conducted with microhardness the focus of the experiment.

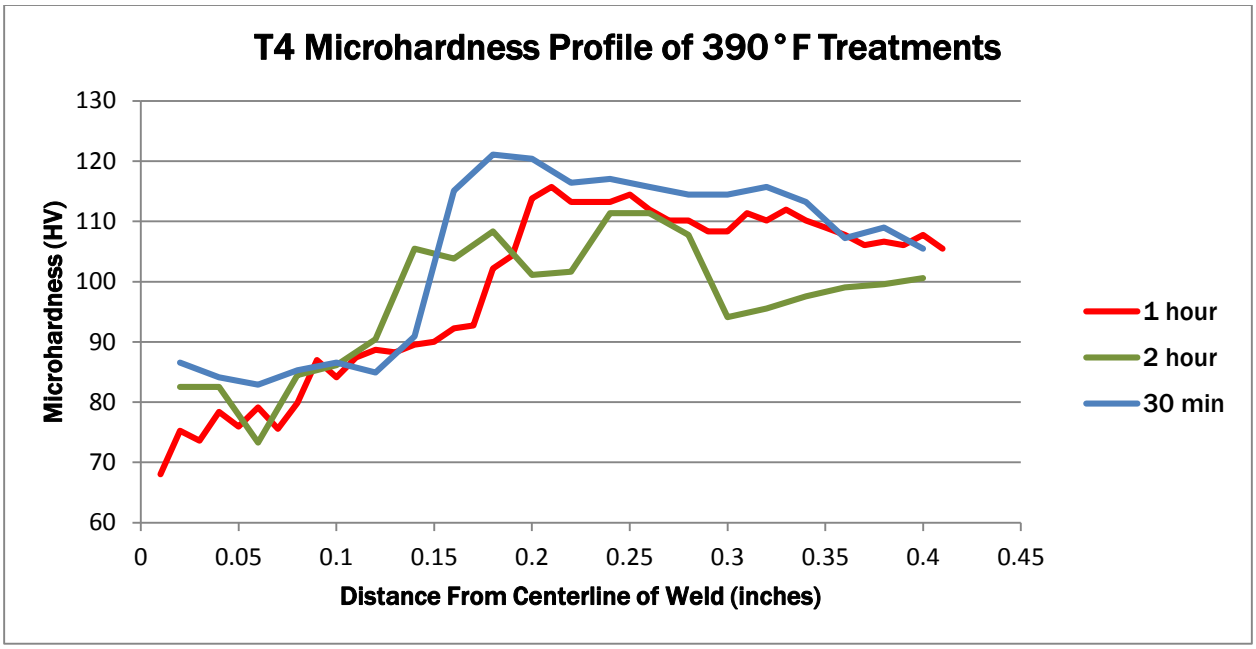

Figure 21 – Overlaid microhardness profiles of T4 samples treated at 390°F display high levels of variance regarding local maximum and minimum HV0.5 values. There is also wide variation in regard to HAZ extent.

4. Discussion

The thermal gradients caused by the process of welding influence the formation and evolution of microstructures present in the base metal. These gradients develop thermal processing histories that are partly a function of distance from the weld midline. Essentially, next to the weld there are regions that reach temperatures near the equilibrium melting temperature and rapidly cool, while regions further away from the weld reach lower temperatures yet cool more slowly. These different thermal histories have a dramatic effect on the microstructures that form or microstructures that were already present.

4.1 Solutionizing of Weld HAZ

Close to the weld, the temperature exceeds the solvus line of Mg-Si in alpha aluminum, around 480°F. This solutionizes the region by dissolving the ß″ back into solution, essentially reversing one of the main processing steps used to strengthen the RX82 alloy (**Figure 7b**). In the T4 samples this re-solutionizing of the HAZ is mitigated through the use of a PWHT. This process enables the precipitates to re-nucleate and grow in the solutionized zone, re-introducing the precipitation hardening mechanism that was used to inhibit dislocation movement and increase the UTS of the extrusion (**Figure 7c**). The T6 samples were not subject to a PWHT, which resulted in the solutionized zone persisting as the welded RX82 extrusions are sent to the

paint-bake cycle. Through the process of exposing the welded T6 to a low temperature environment the solutionized zone undergoes a pseudo PWHT, accomplishing the same general goal of precipitate nucleation and growth.

4.2 Ostwald Ripening

Further away from the weld the thermal gradient is closer to 350°F, instead of over 480°F. This thermal history induces a microstructural evolution that is different from the changes in the solutionized zone. With a temperature rise in the dual phase region, diffusion mechanics are enabled which then promotes thermodynamically driven changes in microstructure. As more atomic movement is enabled, Mg and Si solute present in smaller precipitates and local compositional heterogeneities diffuse towards larger ß′ precipitates in order to reach a lower energy state. The larger precipitates have a smaller surface area to volume ratio than the smaller precipitates, resulting in a lower surface tension and therefore a lower Gibbs free energy. As the average precipitate size increases, there is a corresponding decrease in the total number of precipitates in the system. There is also a change in the crystal structure of the precipitates that makes them completely incoherent from the alpha Al matrix. These two changes result in dislocations being able to move more freely through the system by bowing around the precipitates instead of forcing them to shear through the precipitate. Accordingly, there is a decrease in strength associated with Ostwald Ripening.

The effect of Ostwald Ripening was undoubtedly increased through the sample treatments, however the decrease in strength associated with precipitate solutionizing initially outweighed the decrease in strength from Ostwald Ripening. Further sample treatment recovered strength within the solutionized region while further decreasing the strength of the overaged region; however the decrease in strength from overaging only fell below the re-strengthened solutionized zone when treatment temperature exceeded 390°F, and when the 425°F treatment lasted 2.0 hours instead of 1.0 hour.

5. Conclusions

1. T4 samples showed no statistically significant changes in UTS with changes in thermal treatment temperature or duration.
2. The T6 samples treated at 390°F or 425°F had average UTS values of 34.3 ksi and 32.5 ksi respectively, which were significantly higher than samples treated at 350°F which had average UTS values of 29.8 ksi.
3. The T6 samples treated for 1.0 or 2.0 hours had average UTS values of 33.0 ksi and 33.5 ksi respectively, which were significantly higher than samples treated for 2.0 hours which had average UTS values of 30.1 ksi.

References

[1] Sapa Extrusions, Design Manual: Sucess with Aluminum Profiles, 2009.

[2] Sapa Extrusions, "Extruded Aluminum Alloy 6082," 2012. [Online]. Available: http://www.sapagroup.com/pages/630244/Alloy%206082-%20Rev2012.pdf.

[3] J. Victor, *Metallurgy,* City of Industry: Sapa Profile Academy, 2014.

[4] H. Zhu, M. Couper and A. Dahle, "Effect of Process Variables on Mg-Si Particles and Extrudability of 6xxx Series Aluminum Extrusions," *JOM,* pp. 66-71, 2011.

[5] P. Saha, ""Fundamentals of Extrusion" Aluminum Extrusion Technology," ASM International, Materials Park, 2000.

[6] A. Dustin, *Extrusion Production,* City of Industry: Sapa Profile Academy, 2014.

[7] ASM International, "ASM Specialy Handbook - Aluminum and Aluminum Alloys," 1993. [Online]. [Accessed 31 May 2016].

[8] Lincoln Electric, "A Guide to Aluminum Welding," 27 October 2015. [Online].

[9] S. Missori and A. Sili, "Mechanical Behaviour of 6082-T6 Aluminum Alloy Welds," *Metallurgical Science and Technology,* pp. 12-18, 2000.

[10] Ø. Grong and O. Myhr, "Modeling of Metallurgical Microstructure Evolution in Fusion Welding," *ASM International,* pp. 797-818, 2011.

[11] G. Scamans, P. Andrews, C. Butler, A. Hall and G. Thompson, "Surface Treatment of Aluminum Automotive Sheet," *Surface and Interface Analysis,* pp. 1430-1434, 2013.

[12] P. Sheasby, R. Pinner and S. Wernick, "The Surface Treatment and Finishing of Aluminum and Its Alloys," *ASM International,* 2001.

[13] J. Gossner and K. Tator, "Surface Engineering: Powder Coating," *ASM Handbook,* pp. 421-447, 1994.

[14] J. Holmen, T. Børvik, O. Myhr, H. Fjær and O. Hopperstad, "Perforation of welded aluminum components: Microstructure-based modeling and experimental validation," *Journal of Impact Engineering,* pp. 96-107, 2015.

[15] C. C. LLC, "Factory Chrysler Parts," 2016. [Online]. [Accessed 2016].

[16] ASTM International, "ASTM Standard E384-11E1 - Standard Test Method for Knoop and Vickers Hardness of Materials," West Conshohoken, 2012.

[17] R. Donovan, R. Fortune and R. Trout, "Elevated Temperature Effects on the Mechanical Properties of," DigitalCommons@Calpoly, San Luis Obispo, 2015.

[18] ASTM International, "ASTM B557 - Standard Test Methods of Tension Testing Wrought and Cast Aluminum and Magnesium-Alloy Products," ASTM International, West Conshohocken, PA, 2009.

Appendix A – Tensile Test Data

T4 Tensile Data

Treatment Temperature (°F)	Treatment Time (hr.)	Sample number	Thickness (in.)	Width (in.)	Max Load (Kip)	Max Stress (Ksi)	Average Load (Kip)	Average Stress (Ksi)	Std Dev (Load)	Std Dev (Stress)	% Std Dev Load	% Std Dev Stress
350	0.5	1	0.098	0.495	1.847	38.07	1.86	38.26	0.08	1.47	4.10	3.83
350	0.5	2	0.098	0.495	1.964	40.49						
350	0.5	3	0.098	0.495	1.797	37.04						
350	0.5	4	0.1	0.495	1.920	38.79						
350	0.5	5	0.098	0.495	1.790	36.90						
350	1	1	0.099	0.495	1.921	39.20	1.70	34.91	0.21	4.30	12.59	12.32
350	1	2	0.1	0.495	1.721	34.77						
350	1	3	0.098	0.494	1.660	34.29						
350	1	4	0.098	0.494	1.844	38.09						
350	1	5	0.098	0.494	1.365	28.20						
350	2	1	0.099	0.495	1.903	38.83	1.87	38.24	0.06	1.14	3.22	2.98
350	2	2	0.099	0.495	1.920	39.18						
350	2	3	0.1	0.495	1.918	38.75						
350	2	4	0.098	0.494	1.845	38.11						
350	2	5	0.099	0.495	1.780	36.32						
390	0.5	1	0.098	0.495	1.687	34.78	1.78	36.74	0.07	1.47	3.98	4.00
390	0.5	2	0.098	0.495	1.746	35.99						
390	0.5	3	0.099	0.494	1.795	36.70						
390	0.5	4	0.098	0.495	1.872	38.59						
390	0.5	5	0.098	0.494	1.822	37.64						
390	1	1	0.1	0.495	1.945	39.29	1.85	37.65	0.07	1.24	4.01	3.30
390	1	2	0.098	0.495	1.774	36.57						
390	1	3	0.1	0.494	1.897	38.40						
390	1	4	0.099	0.494	1.843	37.68						
390	1	5	0.099	0.495	1.780	36.32						
390	2	1	0.098	0.494	1.854	38.30	1.85	37.77	0.08	1.44	4.38	3.80
390	2	2	0.098	0.495	1.749	36.05						
390	2	3	0.099	0.495	1.791	36.55						
390	2	4	0.099	0.495	1.883	38.42						
390	2	5	0.1	0.495	1.957	39.54						
425	0.5	1	0.098	0.494	1.754	36.23	1.81	37.10	0.08	1.36	4.21	3.66
425	0.5	2	0.099	0.495	1.742	35.55						
425	0.5	3	0.1	0.495	1.933	39.05						
425	0.5	4	0.099	0.494	1.806	36.93						
425	0.5	5	0.098	0.495	1.830	37.72						
425	1	1	0.1	0.495	1.785	36.06	1.78	36.22	0.03	0.56	1.55	1.54
425	1	2	0.1	0.494	1.797	36.38						
425	1	3	0.099	0.495	1.819	37.12						
425	1	4	0.099	0.495	1.753	35.77						
425	1	5	0.099	0.496	1.757	35.78						
425	2	1	0.098	0.494	1.758	36.31	1.72	35.36	0.04	0.77	2.36	2.19
425	2	2	0.098	0.493	1.662	34.40						
425	2	3	0.099	0.495	1.745	35.61						
425	2	4	0.099	0.495	1.703	34.75						
425	2	5	0.099	0.495	1.751	35.73						

T6 Tensile Data

Treatment Temperature (°F)	Treatment Time (hr.)	Sample number	Thickness (in.)	Width (in.)	Max Load (Kip)	Max Stress (Ksi)	Average Load (Kip)	Average Stress (Ksi)	Std Dev (Load)	Std Dev (Stress)	% Std Dev Load	% Std Dev Stress
350	0.5	1	0.106	0.496	1.455	27.67	1.49	28.39	0.08	1.50	5.33	5.28
350	0.5	2	0.106	0.496	1.608	30.58						
350	0.5	3	0.106	0.496	1.520	28.91						
350	0.5	4	0.106	0.496	1.396	26.55						
350	0.5	5	0.105	0.496	1.471	28.25						
350	1	1	0.104	0.495	1.349	26.20	1.57	30.31	0.14	2.58	8.77	8.50
350	1	2	0.105	0.495	1.614	31.05						
350	1	3	0.104	0.495	1.611	31.29						
350	1	4	0.105	0.495	1.722	33.13						
350	1	5	0.105	0.496	1.555	29.86						
350	2	1	0.106	0.495	1.388	26.45	1.60	30.68	0.26	5.08	16.48	16.55
350	2	2	0.105	0.496	1.744	33.49						
350	2	3	0.105	0.495	1.256	24.17						
350	2	4	0.106	0.495	1.747	33.30						
350	2	5	0.105	0.495	1.870	35.98						
390	0.5	1	0.105	0.496	1.344	25.81	1.61	30.99	0.15	2.91	9.23	9.38
390	0.5	2	0.105	0.496	1.665	31.97						
390	0.5	3	0.104	0.496	1.682	32.61						
390	0.5	4	0.105	0.495	1.687	32.46						
390	0.5	5	0.105	0.495	1.668	32.09						
390	1	1	0.105	0.496	1.763	33.85	1.83	34.99	0.09	1.73	5.06	4.93
390	1	2	0.106	0.495	1.861	35.47						
390	1	3	0.106	0.495	1.901	36.23						
390	1	4	0.106	0.496	1.715	32.62						
390	1	5	0.106	0.496	1.934	36.78						
390	2	1	0.105	0.494	1.984	38.25	1.92	36.78	0.06	1.37	3.26	3.72
390	2	2	0.105	0.494	1.902	36.67						
390	2	3	0.106	0.496	1.818	34.58						
390	2	4	0.105	0.496	1.924	36.94						
390	2	5	0.105	0.496	1.950	37.44						
425	0.5	1	0.105	0.495	1.573	30.26	1.60	30.77	0.08	1.39	5.03	4.51
425	0.5	2	0.104	0.496	1.479	28.67						
425	0.5	3	0.106	0.496	1.663	31.63						
425	0.5	4	0.105	0.496	1.617	31.05						
425	0.5	5	0.105	0.496	1.680	32.26						
425	1	1	0.106	0.497	1.766	33.52	1.75	33.67	0.07	1.54	4.21	4.56
425	1	2	0.105	0.495	1.671	32.15						
425	1	3	0.105	0.495	1.680	32.32						
425	1	4	0.104	0.496	1.783	34.56						
425	1	5	0.104	0.496	1.846	35.79						
425	2	1	0.105	0.496	1.782	34.22	1.72	32.95	0.17	3.24	9.59	9.85
425	2	2	0.106	0.495	1.429	27.23						
425	2	3	0.106	0.495	1.762	33.58						
425	2	4	0.105	0.496	1.801	34.58						
425	2	5	0.105	0.496	1.830	35.14						

Appendix B – Microhardness Data

T4 – 350°F, 0.5 hour Treatment

Distance From Midline (in.)	D1 (microns)	D2 (microns)	D average (microns)	HV0.5
0.01	104.5	105.5	105	84.10
0.02	107	105	106	82.52
0.03	104.5	103.5	104	85.72
0.04	106.5	104	105.25	83.70
0.05	106	106	106	82.52
0.06	107.5	105	106.25	82.13
0.07	105.5	104	104.75	84.50
0.08	105	102.5	103.75	86.14
0.09	103.5	104.5	104	85.72
0.1	105	105	105	84.10
0.11	102	101	101.5	90.00
0.12	101	100.5	100.75	91.34
0.13	99	97.5	98.25	96.05
0.14	88.5	88	88.25	119.05
0.15	87	86.5	86.75	123.21
0.16	87.5	86	86.75	123.21
0.17	87.5	86.5	87	122.50
0.18	88	87.5	87.75	120.41
0.19	88.5	88	88.25	119.05
0.2	88	87.5	87.75	120.41
0.21	89	87.5	88.25	119.05
0.22	88.5	88.5	88.5	118.38
0.23	88.5	88	88.25	119.05
0.24	88.5	88	88.25	119.05
0.25	90	89.5	89.75	115.11
0.26	88.5	88.5	88.5	118.38
0.27	90	88.5	89.25	116.40
0.28	89.5	89.5	89.5	115.75
0.29	88.5	88.5	88.5	118.38
0.3	90	88.5	89.25	116.40
0.31	88	90	89	117.06
0.32	89.5	90	89.75	115.11
0.33	87.5	91	89.25	116.40
0.34	90	89.5	89.75	115.11
0.35	89	89.5	89.25	116.40
0.36	89.5	90	89.75	115.11
0.37	90	90.5	90.25	113.84
0.38	92.5	91.5	92	109.55
0.39	93.5	92.5	93	107.20
0.4	94	92.5	93.25	106.63
0.41	94.5	96.5	95.5	101.66
0.42	95.5	97	96.25	100.09

T4 – 350°F, 1.0 hour Treatment

Distance From Midline (in.)	D1 (microns)	D2 (microns)	D average (microns)	HV0.5
0.01	109	109.5	109.25	77.68
0.02	107	110	108.5	78.76
0.03	107.5	107.5	107.5	80.23
0.04	106	104.5	105.25	83.70
0.05	105.5	104.5	105	84.10
0.06	105.5	107.5	106.5	81.75
0.07	105	104.5	104.75	84.50
0.08	106.5	104.5	105.5	83.30
0.09	109.5	104	106.75	81.37
0.1	105.5	103	104.25	85.31
0.11	104.5	105	104.75	84.50
0.12	103.5	105.5	104.5	84.91
0.13	90	91.5	90.75	112.58
0.14	86.5	88.5	87.5	121.10
0.15	87	89.5	88.25	119.05
0.16	86.5	90.5	88.5	118.38
0.17	87.5	89	88.25	119.05
0.18	87.5	90	88.75	117.72
0.19	88.5	89.5	89	117.06
0.2	87.5	90	88.75	117.72
0.21	88.5	89	88.75	117.72
0.22	87.5	88.5	88	119.73
0.23	89	90	89.5	115.75
0.24	88	89	88.5	118.38
0.25	89	89.5	89.25	116.40
0.26	89.5	89.5	89.5	115.75
0.27	89	89	89	117.06
0.28	89	90	89.5	115.75
0.29	89.5	90	89.75	115.11
0.3	90	92	91	111.97
0.31	91	90.5	90.75	112.58
0.32	91.5	90.5	91	111.97
0.33	91.5	91	91.25	111.35
0.34	93	92.5	92.75	107.78
0.35	93.5	92.5	93	107.20
0.36	92	94	93	107.20
0.37	92	92.5	92.25	108.95
0.38	92.5	95	93.75	105.49
0.39	94	95	94.5	103.83
0.4	95.5	95	95.25	102.20

T4 – 3590°F, 2.0 hour Treatment

Distance From Midline (in.)	D1 (microns)	D2 (microns)	D average (microns)	HV0.5
0.02	106.5	106.5	106.5	81.75
0.04	105	103.5	104.25	85.31
0.06	104	101.5	102.75	87.82
0.08	99	101	100	92.72
0.1	102	102	102	89.12
0.12	100	99	99.5	93.65
0.14	86	85.5	85.75	126.10
0.16	86.5	85.5	86	125.37
0.18	85	86	85.5	126.84
0.2	87.5	86.5	87	122.50
0.22	87	86.5	86.75	123.21
0.24	86.5	86.5	86.5	123.92
0.26	89	88	88.5	118.38
0.28	87.5	88.5	88	119.73
0.3	90	88.5	89.25	116.40
0.32	89	89	89	117.06
0.34	90	91	90.5	113.21
0.36	92	90.5	91.25	111.35
0.38	93.5	93.5	93.5	106.06
0.4	94.5	94.5	94.5	103.83

T4 – 390°F, 0.5 hour Treatment

Distance From Midline (in.)	D1 (microns)	D2 (microns)	D average (microns)	HV0.5
0.02	104	103	103.5	86.56
0.04	103.5	106.5	105	84.10
0.06	104.5	107	105.75	82.91
0.08	105.5	103	104.25	85.31
0.1	102	105	103.5	86.56
0.12	105.5	103.5	104.5	84.91
0.14	102	100	101	90.89
0.16	90	89.5	89.75	115.11
0.18	88	87	87.5	121.10
0.2	87.5	88	87.75	120.41
0.22	89.5	89	89.25	116.40
0.24	89	89	89	117.06
0.26	89.5	89.5	89.5	115.75
0.28	90.5	89.5	90	114.47
0.3	91	89	90	114.47
0.32	88.5	90.5	89.5	115.75
0.34	92	89	90.5	113.21
0.36	93.5	92.5	93	107.20
0.38	92	92.5	92.25	108.95
0.4	93	94.5	93.75	105.49

T4 – 390°F, 1.0 hour Treatment

Distance From Midline (in.)	D1 (microns)	D2 (microns)	D average (microns)	HV0.5
0.01	114.5	119	116.75	68.02
0.02	112	110	111	75.25
0.03	110.5	114	112.25	73.59
0.04	110.5	107	108.75	78.40
0.05	111	110	110.5	75.94
0.06	109	107.5	108.25	79.13
0.07	112.5	109	110.75	75.59
0.08	105.5	110	107.75	79.86
0.09	103	103.5	103.25	86.97
0.1	105	105	105	84.10
0.11	103	103	103	87.40
0.12	101	103.5	102.25	88.68
0.13	103.5	101.5	102.5	88.25
0.14	104	99.5	101.75	89.56
0.15	101	102	101.5	90.00
0.16	99	101.5	100.25	92.26
0.17	99.5	100.5	100	92.72
0.18	95.5	95	95.25	102.20
0.19	94.5	94	94.25	104.38
0.2	91.5	89	90.25	113.84
0.21	91	88	89.5	115.75
0.22	92.5	88.5	90.5	113.21
0.23	92	89	90.5	113.21
0.24	92	89	90.5	113.21
0.25	90.5	89.5	90	114.47
0.26	93	89	91	111.97
0.27	93.5	90	91.75	110.14
0.28	93	90.5	91.75	110.14
0.29	93	92	92.5	108.37
0.3	93.5	91.5	92.5	108.37
0.31	91	91.5	91.25	111.35
0.32	93	90.5	91.75	110.14
0.33	91.5	90.5	91	111.97
0.34	93	90.5	91.75	110.14
0.35	94	90.5	92.25	108.95
0.36	94.5	91	92.75	107.78
0.37	96	91	93.5	106.06
0.38	94	92.5	93.25	106.63
0.39	95.5	91.5	93.5	106.06
0.4	94	91.5	92.75	107.78
0.41	96	91.5	93.75	105.49

T4 – 390°F, 2.0 hour Treatment

Distance From Midline (in.)	D1 (microns)	D2 (microns)	D average (microns)	HV0.5
0.02	103.5	108.5	106	82.52
0.04	107	105	106	82.52
0.06	112.5	112.5	112.5	73.26
0.08	105.5	104	104.75	84.50
0.1	102	105.5	103.75	86.14
0.12	102	100.5	101.25	90.44
0.14	94	93.5	93.75	105.49
0.16	95	94	94.5	103.83
0.18	91.5	93.5	92.5	108.37
0.2	96	95.5	95.75	101.13
0.22	95.5	95.5	95.5	101.66
0.24	91.5	91	91.25	111.35
0.26	92	90.5	91.25	111.35
0.28	94	91.5	92.75	107.78
0.3	100	98.5	99.25	94.13
0.32	99	98	98.5	95.57
0.34	98	97	97.5	97.54
0.36	97.5	96	96.75	99.05
0.38	97.5	95.5	96.5	99.57
0.4	96.5	95.5	96	100.61